INVESTIGATION OF THE STRUCTURE OF STRATIFIED FLOWS BY THE METHOD OF LASER SCANNING

E. V. Gumennik and Yu. D. Chashechkin

UDC 53.082.25

The main features of turbulent and rotational motions in a stratified medium are anisotropy of transfer in the vertical and horizontal directions, caused by the action of buoyancy forces, and formation of layered structures [1]. The mechanisms of formation, the laws of evolution, and the degeneracy of the structures have not been adequately studied. One reason for this is that experimental methods and means for measuring the fine structure of the distribution of the density in stratified media have not been adequately developed.

Contact-free optical methods are widely employed for the experimental study of the density structure of stratified flows. In particular, significant results have been obtained by shadow methods; with those methods, however, it is difficult to organize real-time information processing using modern measuring instruments.

Laser scanning refractometers (LSRs), based on electric recording of the instantaneous value of the angle of refraction of a narrow scanned laser beam, probing the object under study [2, 3], make it possible to obtain real-time quantitative information about the density structure of the object. Like in shadow methods, the parameter measured is the gradient of the index of refraction integrated over the length of the probing beam. But here information is obtained not in the form of the distribution of the illumination in the plane of the shadow image of the object, but rather in the form of an electrical signal; this makes possible direct use of modern instrumentation, in particular, computers, for information processing [4].

At the present time, however, only LSRs with linewise scanning have been realized [2, 4]. This is connected with technical difficulties in fabricating the corresponding X–Y scanners, necessary for organizing framewise scanning in LSRs. To expand the capabilities of laser scanning systems with linewise scanning LSRs must be combined with traditional shadow devices [4], but the possibilities for optimizing the parameters of LSRs are limited, in this case, by the constructional features, the dimensions, and the optical characteristics of serially produced shadow apparatus. Thus the spatial resolution of an LSR combined with an IAB-458 apparatus [4] is determined by the size of the probing beam in the object under study $w_0 = \lambda f_s/\pi w$ (λ is the wavelength of the laser radiation, w is the size of the laser beam on the scanner, f_s is the focal length of the main objective of the shadow apparatus) and cannot be made small enough owing to the large values of f_s.

In this paper we present the results of the development of a measuring system in which a laser shadow apparatus (SA) is combined with an LSR. The common source of light is a laser and it is possible to vary independently the parameters of the LSR and the SA; in addition, the results obtained using this system can be used to study the structure of the stratified flow downstream from a blunt cylinder.

The experiments were performed in a small (60 × 10 × 20 cm) laboratory basin made of plexiglass. The blunt cylindrical body was pulled along the axis of symmetry of the basin. Linear stratification was created by the method of continuous displacement [5] by changing the concentration of the water solution of sodium chloride along the vertical direction. Three values of the period of buoyancy $T_* = 2\pi/N = 2\pi(g/\Lambda)^{1/2}$, calculated from the filling, were used: 3.5, 4.9, and 9.8 sec. Here N is the frequency of buoyancy; g is the acceleration of gravity; $\Lambda = (d \ln \rho/dz)^{-1}$ is the scale of variation of the density in the undisturbed medium; ρ is the density; and, z is the vertical coordinate in the direction g. In addition, two pulling regimes with different velocities U, for which the values of the Reynolds numbers were calculated for the diameter of the cylinder d Re = 650 and 1300, were employed. These conditions made it possible to perform experiments with internal Froude numbers $Fr = U^2\Lambda/gd^2$ = 4.6; 9.0; 18.4; 36.0; 144.0.

Moscow. Translated from Zhurnal Prikladnoi Mekhaniki i Tekhnicheskoi Fiziki, No. 2, pp. 177-182, March-April, 1990. Original article submitted November 15, 1988.

0021-8944/90/3102-0333$12.50

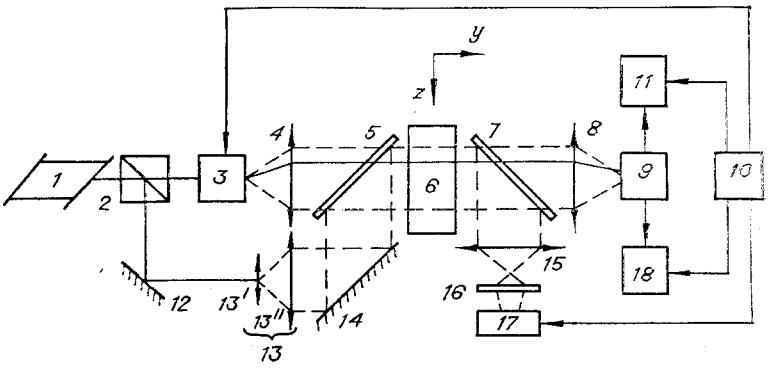

Fig. 1

The structural arrangement of the LSR with linewise scanning of the probing beam along the vertical and the laser SA combined with it is presented in Fig. 1. The LSR includes a laser 1, a scanner 3, an illuminator 4, a receiving objective 8, a position-sensitive photodetector (PSP) 9, auxiliary apparatus, which included a spectrum analyzer 11 and an automatic plotter 18, and a synchronization unit 10. The laser beam scanner is a mirror whose angle of inclination is controlled with the help of an electrical signal and is located in the front focal plane of the illuminating objective. In operating the scanner the laser beam probing the object under study 6 is moved in a plane-parallel fashion. The PSP consists of two photodiodes on a common substrate, separated by a narrow boundary and connected in a differential arrangement [6], and is placed in the back focal plane of the receiving objective. Thus, with accuracy up to aberrations of the optical system of the LSR and in the absence of nonuniformities of the index of refraction n, caused by perturbations of the density in the volume being probed, a zero signal is obtained at the output of the PSP in the entire scanning range. When the object under study is scanned the electric signal u at the output of the PSP at each moment in time t is determined by the value of the gradient of the density integrated over the length of the probing beam at the corresponding time t according to the scanning law $z = \varphi(t)$:

$$u(t) = Bf_2 \frac{0.231}{n_0} \int_0^L \frac{\partial \rho}{\partial z} dy.$$

Here B is the slope of the coordinate characteristic of the PSP [6]; f_2 is the back focal length of the receiving objective of the LSR; n_0 is the index of refraction of the medium surrounding the object under study; and, L is the size of the working part along the direction y. Neglecting the dispersion of the index of refraction of the solution of sodium chloride, it was assumed that $n = 1.1020 + 0.231\rho/\rho_0$ [7] (ρ_0 is the density of water at 4°C).

For sufficiently fast scanning, when the line-scan time is shorter than the characteristic time τ over which the density changes in the flow under study, the frequency structure of the signal u(t) corresponds, with accuracy up to the spatial resolution of the LSR, to the spatial structure of the quantity $R(z) = \int_0^L (\partial\rho/\partial z)dy$, and for a two-dimensional object, when $\rho \neq \varphi(y)$, it corresponds to the quantity $R_0(z) = L\partial\rho/\partial z$. A more detailed description of the operation of the LSR as well as analysis of its working characteristics are presented in [3, 4].

The shadow apparatus includes a laser 1, a beam-splitting cube 2, a system 13, consisting of a microobjective 13' and a objective 13'' with a long focal length for expanding the beam, rotating mirrors 12 and 14, a receiving object 15, a screen 16, and a motion picture camera 17. The parallel beam of coherent light, forming after the laser radiation is transformed by the system 13, illuminates the object. The fluctuations of the index of refraction (density) in the object give rise to refraction of the light at the output from the object by an angle $\theta_z = \frac{1}{n_0} \int_0^L (\partial n/\partial z)dy$, which with the help of the receiving objective is converted into the redistribution of the illumination on the screen, forming a shadow pattern.

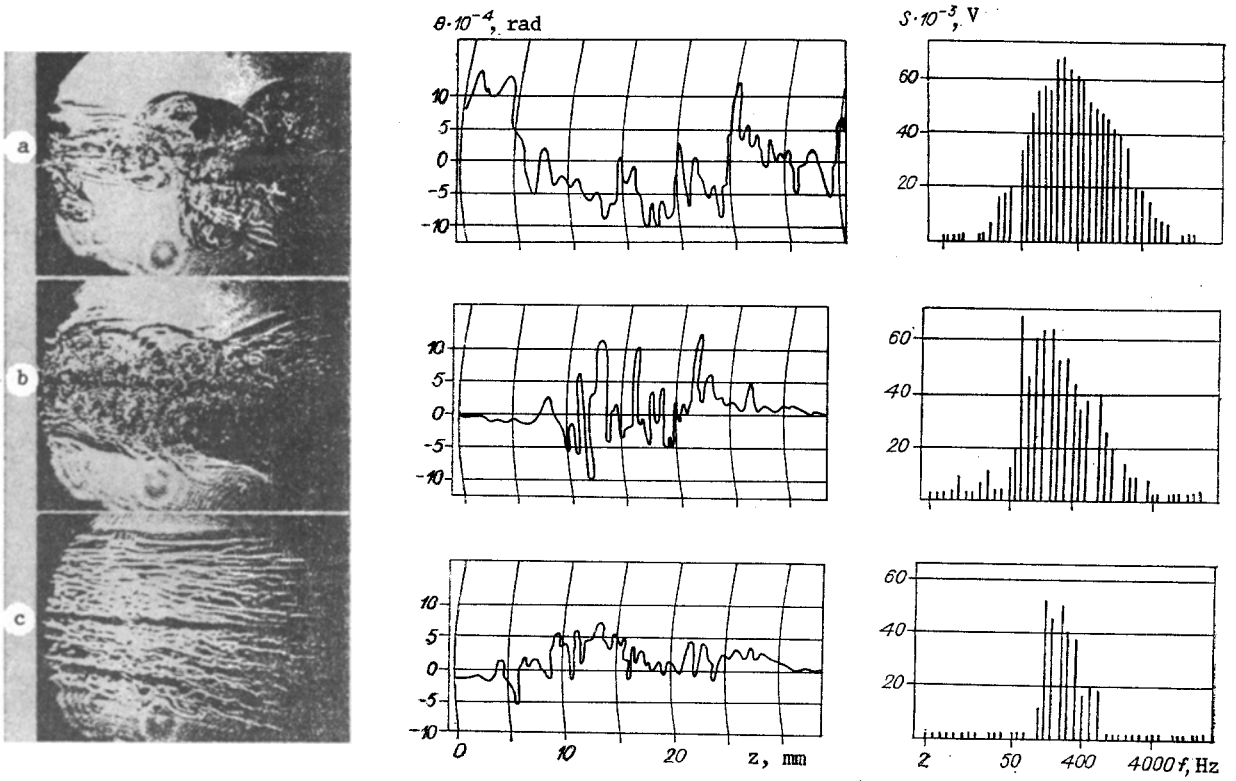

Fig. 2

The shadow apparatus is combined with the LSR with the help of two plane-parallel half-transmitting plates 5 and 7. The shadow pattern permits representing the structure of the flow as a whole, and with the help of the LSR combined with the SA it makes it possible to obtain under controllable conditions quantitative information about the vertical distribution of the density gradient. Since the system was created for measuring the parameters of the fine structure, the SA was constructed for recording $\partial^2 n/\partial z^2$. This made it possible to eliminate the effect of the fine structure of density disturbances caused by internal waves on the shadow pattern. The operating mode of the SA (adjustment of SA for measuring $\partial n/\partial z$) is performed by inserting a visualizing diaphragm in the focal plane of the objective.

Figure 2 shows the shadow patterns of the comoving flow downstream from the pulled cylinder at different times with Re = 1300 and Fr = 36 and the corresponding records of the signals of the LSR, which were obtained synchronously with the shadow patterns and represent the "instantaneous" profiles of the vertical distribution of the gradient of the density in the comoving flow as well as their spectra. Figure 2a corresponds to the moment $\tau = t/T_* = 0.5$, Fig. 2b corresponds to $\tau = 1$, and Fig. 2c corresponds to $\tau = 5$, where the time t is measured from the moment the pulled body passes through the scanning plane coinciding with the central section of the shadow pattern. The signal records were obtained with the help of a fast N338 automatic plotter and the spectra were obtained with the help of a spectral analyzer of the parallel type FSP-80, whose operation was synchronized with that of the scanner.

One can see in Fig. 2 that the results presented in the form of the shadow pattern correspond well to the LSR signal and its spectrum. Thus at the early stage of development (a) the flow is characterized by the presence of significant long-period disturbances of the density and a wide spectrum of their spatial scales. As the flow evolves the absolute values of the density gradient decrease and the spectrum of the spatial scales (b) becomes narrower. The distribution shown in Fig. 2c is characterized by deviations of the density gradient that have a small amplitude and are quite regular along the vertical coordinate; this is typical for a layered structure of the vertical distribution of the density, forming with the evolution of the comoving flow in a stratified medium.

The transformation of the form of the spectrum from symmetric to unsymmetric and bimodal (see Figs. 2a-c, respectively) can be explained by the specific nature of the process of energy transfer along the spatial spectrum in a stratified flow. However this question requires a more detailed analysis, since the indicated transformation of the spectrum could be

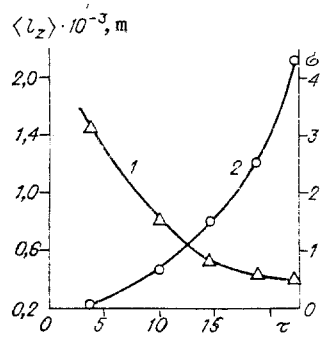

Fig. 3

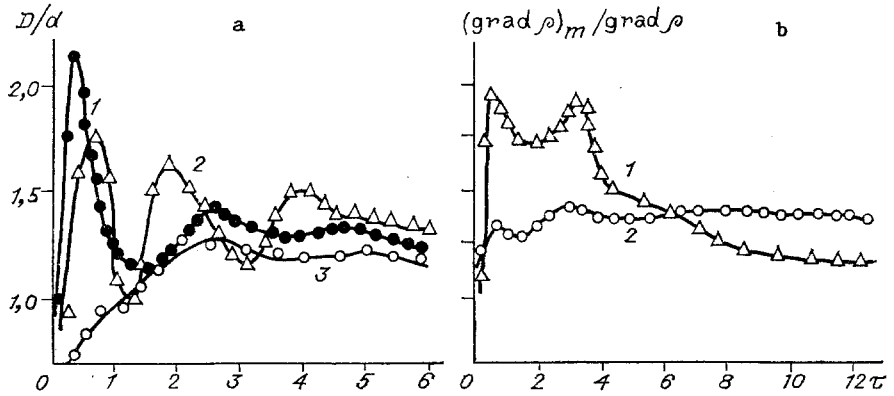

Fig. 4

of an instrumental nature, which is connected with the instrumental enhancement of the high-frequency (short-period) part of the spectrum owing to the limited spatial resolution of the LSR. Thus in the measurements performed the characteristic size of the probing laser beam is ~ 0.15 mm and the density nonuniformities with scales $\lesssim$ 0.15 mm cause the apparatus to respond not to the refraction of the probing beam as a whole (geometric-optics approximation) but rather diffraction of the probing beam by fine-scale fluctuations of the density.

Figure 3 shows the dependences obtained by spectral analysis of the LSR signals, consisting of the time dependences of the average size $\langle l_z \rangle$ of the nonuniformities of the vertical profile of the density gradient (curve 2) and the relative spread σ in the sizes of these nonuniformities around the average value (curve 1). Here Re = 1300, Fr = 36, and

$$\langle l_z \rangle = v \left(\frac{\sum_{i=1}^{k} S_i f_i \Delta f_i}{\sum_{i=1}^{k} S_i \Delta f_i} \right)^{-1},$$

$$\sigma = \left(\frac{\sum_{i=1}^{k} S_i (v/f_i - \langle l_z \rangle)^2 \Delta f_i}{\sum_{i=1}^{k} S_i \Delta f_i} \right)^{1/2},$$

where v is the rate of scanning of the probing laser beam; S_i is the measured spectral component of the LSR signal; f_i and Δf_i are the central frequency and transmission band of the i-th filter of the FSP-80 spectrum analyzer, which operates by the principle of multichannel filtering and has 38 (i = 1, 2, ..., k = 38) parallel filters, covering the frequency band 1.5 Hz-22.4 kHz.

Figure 4 shows the dependences of the vertical size of the comoving flow D (a) and the maximum value of the vertical component of the density gradient $(\mathrm{grad}\,\rho)_m$ in it (b) versus the dimensionless time τ with Re = 1300 obtained as a result of the analysis of the LSR data. Here $(\mathrm{grad}\,\rho)_0$ characterizes the initial stratification of the undisturbed medium. Analysis

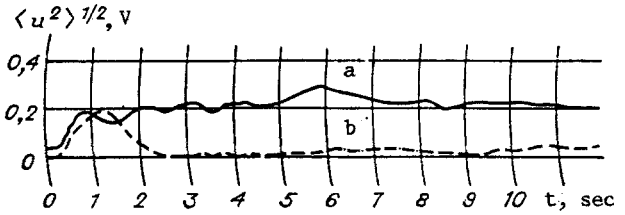

Fig. 5

of the data shows that for larger Fr intense mixing of liquid, occurring by means of large-scale eddies (see Figs. 2a, 3, and 4b), occurs in the comoving flow studied. The nonequilibrium density distribution forming in the process collapses under the action of buoyancy forces (Fig. 4a); we note that for the weakest of the stratifications studied (Fr = 144.0) the value found for the time at which collapse starts $\tau_* = 0.3$ (curve 1) agrees with the data of [8, 9]. For stronger stratification (Fr = 36.0) collapse starts later and $\tau_* = 0.5$ (curve 2). This can be explained by the fact that the stronger stratification suppresses large-scale eddies more efficiently, as a result of which mixing occurs more slowly in the comoving flow and the effect of buoyancy forces is manifested later. This is confirmed also by the behavior of the dependence 3 shown in Fig. 4a, corresponding to the strongest of the stratifications studied, as well as by comparing the dependences 1 and 2 presented in Fig. 4b.

We note that the maximum density gradient obtained with Re = 1300 and Fr = 36.0 in the interlayers is approximately two times greater than the value characterizing the initial stratification. The decrease in $(\text{grad } \rho)_m$ at $\tau \sim 2$ and the increase at $\tau \sim 3.5$ (see Fig. 4b, curve 1) are related with the corresponding increase and decrease of the width of the comoving flow (see Fig. 4a, curve 2).

The method of laser scanning was also used to study the relaxation of the vertical profile of the density gradient, perturbed by the comoving flow, to the starting state. Rapid scanning of the object was employed, and the signal from the output of the PSP was fed into an rms voltmeter. The averaging time of the voltmeter was set to be much greater than the line-scan time, and in the experiments performed it was equal to 0.3 sec with a scanning frequency of 30 Hz. The quantity $\langle u^2 \rangle^{1/2}$, equal to the density of the signals at the output of the voltmeter when scanning the object $\langle u_s^2 \rangle^{1/2}$ and when scanning the starting stratification $\langle u_0^2 \rangle^{1/2}$, was used as the quantitative characteristic of the deviation of the vertical profile of the density gradient from the starting state and was recorded with the help of an automatic plotter.

The results of an investigation showed that after the active stage of the motion is completed the vertical profile of the density gradient in the medium differs for a long time from the starting profile. This difference disappears slowly because it is determined by slow advection and molecular diffusion processes. Figure 5 shows records of the signals at the output of the rms voltmeter with Re = 1300 and Fr = 36.0 (a) and Re = 650 and Fr = 36.0 (b). It should be noted that the difference between the vertical profile of the density gradient and the background level $\langle u_0^2 \rangle^{1/2}$ is also observed at significantly longer times than those shown in Fig. 5. Thus for the comoving flow characterized by the parameters Re = 1300 and Fr = 18.4 such a difference was reliably recorded at times $\sim 5 \cdot 10^3$ sec.

Thus the combined scanning of a narrow laser beam with shadow methods makes it possible to study effectively the dynamics of the density structure of stratified flows. In this method stringent requirements are not imposed on the optical quality of the basin and the method is quite versatile.

LITERATURE CITED

1. J. Turner, Buoyancy Effects in Fluids; Cambridge Univ. Press, New York (1973).
2. E. V. Gumennik and B. S. Rinkevichyus, "Laser scanning refractometer for thermophysical studies," Teplofiz. Vys. Temp., 23, No. 4 (1985).
3. E. V. Gumennik, O. A. Evtikhieva, B. S. Rinkevichyus, and Yu. D. Chashechkin, "Combined use of qualitative and quantitative refractometric methods," Inzh.- Fiz. Zh., 50, No. 4 (1986).
4. E. V. Gumennik and B. S. Rinkevichyus, "The use of refraction of a scanned laser beam for studying the structure of transparent nonuniformities," Teplofiz. Vys. Temp., 25, No. 6 (1987).

5. G. Oster, "Density gradients," Sci. Am., 212, No. 12 (1965).
6. L. S. Aĭvazova, T. Ya. Gorbach, K. M. Krolevets, and V. N. Savelov, "Four-element position-sensitive photodiodes" in: Semiconductor Technology and Microelectronics [in Russian], Naukova Dumka, Kiev (1966).
7. D. E. Mowbray, "The use of schlieren and shadowgraph techniques in the study of the flow patterns in density stratified," J. Fluid Mech., 27, No. 3 (1967).
8. A. H. Schooley, "Wake collapse in a stratified fluid," Science, 157, No. 3787 (1967).
9. G. E. Merritt, "Wake growth and collapse in stratified flow," AIAA J., 12, No. 7 (1974).

CURRENT CONTROL WITH A VARIABLE INDUCTANCE

P. I. Zubkov, L. A. Luk'yanchikov, and K. A. Ten

UDC 533.95:537.84

A number of authors [1-3] point out correctly that the inductance of the commutator circuit, which extracts energy from the accumulator into the load, is "parasitic." Indeed, the voltage on the commutator in the simplest electrotechnical model (Fig. 1) is given by the expression

$$U_b = U_\ell + L_\ell \dot{I}_\ell - MI - L_b \dot{I}_b = V_\ell - M\dot{I} - L_b \dot{I}_b.$$

Here the indices b and ℓ denote quantities referring to the circuit of the circuit breaker and the load; L_b, L_ℓ, and M are the inductance and mutual inductance of the accumulator and load circuits; the dot denotes, as usual, a derivative with respect to the time; U_b and U_ℓ are, in the general case, the nonlinear characteristics of the commutator and the load unrelated with their inductances; and, V_ℓ is the voltage on the load.

For successful operation of the commutator $\dot{I}_b < 0$, $\dot{I} < 0$, whence it follows that $U_b \geq V_\ell$, and in addition the equality obtains at the moment when the switching of the current ends. Further, since the current in the commutator varies from the maximum value to zero and in the load from zero up to the maximum value, it follows from the inequality of the voltages that at the starting stage of switching the power dissipated by the commutator must exceed the power released in the load and in some cases its maximum value also. Thus the inductance in the commutator circuit makes more stringent the conditions of operation of the commutator. For $M < 0$, which in the case of inductive energy accumulators, can always be made to be satisfied constructionally, the operating conditions of the commutator are eased somewhat. In magnetic cumulation generators this condition cannot always be satisfied.

This is the case when the inductance of the commutator circuit is constant or changes very little. When it changes significantly the picture of the process can be completely different. Switching of the current is possible in this case by virtue of the fact that there arises on the varying inductance an emf ($\varepsilon = -d(LI)/dt$) that permits controlling the current. In explosive magnetic generators a varying inductance is employed to obtain high currents, magnetic fields, and energies [4-6].

The purpose of this work is to show that the current in different electrical circuits can be controlled with the help of both varying and increasing inductances. This method of current control has a number of advantages over, for example, current breakers. They include the absence of dissipation (arcing) of energy in the medium (which destroys its initial electrophysical properties), the possibility of current control according to a presented law, etc.

We shall consider some simple electrotechnical models of circuits employed in pulsed power engineering to obtain high powers. We shall not be concerned with the reasons for the change in the commutating inductance, since they can be diverse and unique to each specific case. In addition, we shall neglect Joule losses, making the assumption that the conductors are perfect.

1. We shall study current control by the commutating inductance in extracting energy from an accumulator into an inductive load for the scheme (Fig. 1) employed by Knopfel [7]

Novosibirsk. Translated from Zhurnal Prikladnoi Mekhaniki i Tekhnicheskoi Fiziki, No. 2, pp. 182-187, March-April, 1990. Original article submitted November 29, 1988.

 0021-8944/90/3102-0338$12.50